Basic

European Journal of Immunology

Immunodeficiencies and autoimmunity

Research Article

Genetic dissection of a major haplotype associated with arthritis reveal FcγR2b and FcγR3 to act additively

Daniëlle Vaartjes[1], Dorota Klaczkowska[1], Mark S Cragg[2], Kutty Selva Nandakumar[1,3], Liselotte Bäckdahl[1] and Rikard Holmdahl[1,3]

[1] Division of Medical Inflammation Research, Department of Medical Biochemistry and Biophysics, Karolinska Institute, Stockholm, Sweden
[2] Antibody and Vaccine Group, Centre for Cancer Immunology, University of Southampton Faculty of Medicine, Southampton, UK
[3] SMU-KI United Medical Inflammation Center, School of Pharmaceutical Sciences, Southern Medical University, Guangzhou, China

A haplotype with tightly linked Fc gamma receptor (FcγR) genes is known as a major locus controlling immune responses and autoimmune diseases, including arthritis. Here, we split a congenic fragment derived from the NOD mouse (*Cia9*) to study its effect on immune response and arthritis in mice. We found that arthritis susceptibility was indeed controlled by the FcγR gene cluster and a recombination between the FcγR2b and FcγR3 loci gave us the opportunity to separately study their impact. We identified the NOD-derived FcγR2b and FcγR3 alleles as disease-promoting for arthritis development without impact on antibody secretion. We further found that macrophage-mediated phagocytosis was directly correlated to FcγR3 expression in the congenic mice. In conclusion, we positioned FcγR2b and FcγR3 alleles as disease regulatory and showed that their genetic polymorphisms independently and additively control innate immune cell activation and arthritis.

Keywords: collagen-induced arthritis · Fc gamma receptor · *Cia9* locus · FcγR2b · FcγR3

Additional supporting information may be found online in the Supporting Information section at the end of the article.

Introduction

The etiology of chronic autoimmune diseases, such as rheumatoid arthritis (RA) and systemic lupus erythematosus (SLE), are polygenic diseases with numerous loci, each with small effects. However, a tightly linked region including the low-affinity FcγR genes has shown clear importance [1,2].

Linkage analyses in mouse models have revealed a major regulatory effect from a locus on chromosome 1 containing low-affinity FcγR genes (*Cia9*), associated with both antibody production and disease severity [3,4]. However, identification of the underlying gene variants has so far been unsuccessful. The problem with this region on chromosome 1 is its high density of polymorphic genes in both mice and humans, of which many genes can have potential importance for the regulation of chronic inflammation [5, 6]. Despite the strong genetic association to autoimmune diseases in this region, no specific FcγR encoded polymorphisms have been identified as disease causative. Instead, the autoimmune disease regulatory function of FcγRs has been mostly studied using different KO mouse models, which has led to some confusion. One problem has been linked genes from

Correspondence: Rikard Holmdahl
e-mail: rikard.holmdahl@ki.se

embryonic stem (ES) cells. Studies with FcγR2b KO mice show that the surrounding genes rather than *FcγR2b* regulate immune response [6–8]. Even when syngenic ES cells are used, effects from genetic manipulation can be seen [9], which makes it difficult to mimic the naturally selected polymorphisms that could regulate disease. Analyzing the individual effect from this composite set of highly polymorphic genes can therefore better be assessed in a more biological setting through natural polymorphisms by genetic mapping of phenotypic associations to relevant inflammatory disorders [5,10–12].

Previous studies pinpointed the *Cia9* locus on chromosome 1 as being the major locus besides the MHC region to be associated with collagen-induced arthritis (CIA) [3], the classical mouse model for RA. The association of *Cia9* with arthritis was confirmed using a genome-wide mouse heterogeneous stock analysis, with the contribution of eight inbred mouse strains [13,14]. CIA severity and the levels of anti-CII antibodies were significantly increased in a B10.Q mouse with a NOD-derived *Cia9* congenic fragment, which included the FcγR locus [3].

Here, we aimed to better understand the genetic control of chronic inflammation in the *Cia9* region by positioning the causative gene(s). We have established four informative overlapping sub-congenic *Cia9* strains (*Cia9b, Cia9c, Cia9i*, and *Cia9k*), identifying the FcγR gene cluster and allowing to dissect the function of FcγR2b and FcγR3 independently of each other. We found that *FcγR2b* and *FcγR3* genes additively control inflammatory responses and arthritis.

Results

Congenic mapping of Cia9 identified the arthritis regulatory region to a <1Mb fragment

We have previously shown that a chromosome 1 congenic locus (*Cia9*, 10 Mb in length) from NOD mice introgressed onto the B10.Q background mediates increased susceptibility to CIA [3,14]. To identify the underlying loci, we further refined the locus and established four overlapping *Cia9* sub-congenic mouse strains (*Cia9b, Cia9c, Cia9i*, and *Cia9k*).

The *Cia9b* fragment covers the region above the FcγR gene cluster, whereas *Cia9c* covers the region below the FcγR gene cluster and contains several genes from the signaling lymphocyte activation molecule (SLAM) family, in which polymorphisms have been shown important in maintaining tolerance in lupus [6,10]. The *Cia9i* fragment contains the highly polymorphic NOD-derived FcγR gene cluster, consisting of *FcγR2b*, *FcγR4*, and *FcγR3*. The smaller *Cia9k* fragment harbors NOD *FcγR2b* and *FcγR4* alleles (Fig. 1).

We then tested which of the recombinant congenic fragments conferred the arthritis susceptibility seen in the original *Cia9* fragment by using the type II collagen (CII) specific T and B cell-dependent CIA model, as well as the T and B cell-independent collagen antibody-induced arthritis (CAIA) model [15,16]. No differences in arthritis development were observed between *Cia9b* or *Cia9c* congenic mice and WT mice (Supporting Information Fig. S1), restricting the disease-regulating interval to less than 1 Mb of the *Cia9* locus, i.e., the Cia9i congenic containing the FcγR cluster.

After screening a high number of meiosis, we obtained a recombination within the FcγR gene cluster, excluding the NOD *FcγR3* allele from the fragment (*Cia9k),* (Fig. 1). To investigate the role of the different Fc**γ**Rs in arthritis development, CIA was induced in WT, *Cia9i*, and *Cia9k* mice, and in FcγR2b KO and FcγR3 KO mice for experimental control (Fig. 2A and B). In agreement with previous studies, Fc**γ**R2b KO mice developed severe arthritis, whereas Fc**γ**R3 KO mice were completely resistant [17–20]. Due to disease severity, FcγR2b KO mice had to be sacrificed before the second injection with CII. Compared to WT mice, *Cia9i* congenic mice developed more severe arthritis with earlier disease onset. The arthritis severity of *Cia9k* mice was milder than *Cia9i* mice, but more severe compared to WT mice. Despite these differences, similar serum levels of anti-CII antibodies were analyzed in the congenic mice at day 21 and 57 after immunization (Fig. 2C–E). The serum levels of anti-CII IgG2b were elevated in *FcγR2b* KO mice, but which was related to arthritis severity rather than a direct effect on B cell response.

In summary, mice carrying the NOD-derived *FcγR* gene cluster (*Cia9i*) or a part of the *FcγR* gene cluster (*Cia9k*) were more susceptible to CIA arthritis disease development compared to WT mice, whereas no differences in antibody levels were observed. Therefore, these results show that FcγR2b and FcγR3 act in concert to determine the magnitude of inflammatory effector cell responses.

Conserved FcγR haplotypes

Aiming to study variations in a multiple genome comparison across the *FcγR* genes, public data from the Welcome Trust mouse genome project was assessed that consists of 30 common laboratory strains, including the reference genome (C57BL/6J), and 7 wild mouse strains [21,22]. A total of 4020 SNPs was found in the *FcγR* region (170.9–171.07) that differed between the 37 strains. *Mus Spretus* and *Mus Castaneus* were the strains that differed the most, as expected, since they are distant from *Mus Musculus* strains. In fact, 1920 out of the 4020 SNPs were unique to either *Mus Spretus* or *Mus Castaneus* or were only shared by the two. Looking closer at the remaining 2100 SNPs in the *FcγR* region, 1239 SNPs (of which 9 are non-synonymous coding) separated the 35 strains into two distinct haplotype regions covering *FcγR2b* and *FcγR4* (Supporting Information Table S1). Twelve mouse strains, including C57BL/10J and the reference genome, shared haplotype I derived from the *M. musculus molossinus* (MOLF/EiJ). The *M. musculus musculus derived* haplotype, haplotype II, was shared by 22 mouse strains including NOD and four wild mouse strains

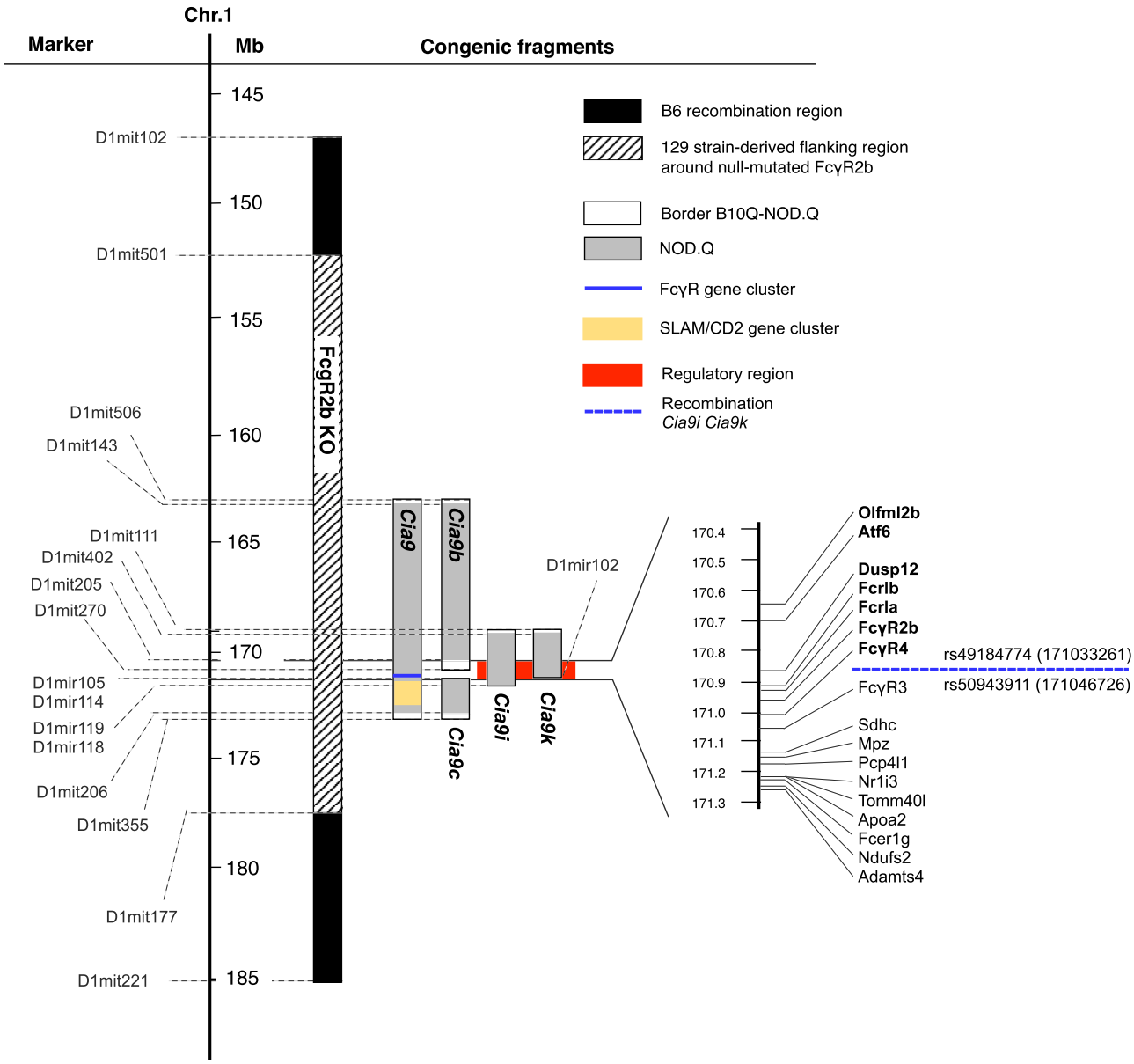

Figure 1. Overview of the *Cia9* sub-congenic fragments compared to Fcγ2b KO mice. The positional information of the *FcγR2b* KO mice was adapted from [7]. The locations, indicated in mega base pairs (Mb), are based on the mouse genome assembly GRCm38/mm10. The different bars represent different fragments. The borders of the congenic fragments are defined by the respective markers, and the region outside applies to the B10.Q background. *Cia9* (163.5-173), *Cia9b* (163.5-170.4), *Cia9c* (171.3-173.0), *Cia9i* (169.3-171.5), *Cia9k* (169.3-171.0). Within the *Cia9* fragment, the FcγR and SLAM/CD2 gene clusters are highlighted. The arthritis regulatory region (≤1Mb), with corresponding protein-coding genes, is indicated in red. The dashed blue line shows the recombination between *Cia9i* and *Cia9k*, identified by the corresponding SNPs (rs49184774 and rs50943911, sequenced using primer pair 1 (F: TGATTGTTGCCAGGGCTAGG, R: AATGAACCTCCTCTGCAGGC) and primer pair 2 (F: CTGCTGGGTGAAACAAAGGC, R: AGATGGCGGTACTAGGGTGT), respectively). The genes in bold are located in the *Cia9k* fragment, whereas the rest was contained within the *Cia9i* fragment.

(Supporting Information Table S1). In the six laboratory strains carrying alleles from haplotype I upstream of *FcγR3*, a recombination has occurred with a change to haplotype II: the BALBc, CBA, two DBA strains, and two B57 strains, suggesting that the haplotype polymorphism was selected in the wild mouse population. This suggests that the haplotypes, now splitted in our congenic strains, have been conserved by strong natural selection.

Polymorphisms of the FcγR cluster regulate the inflammatory arthritis effector phase

To examine the inflammatory and not autoimmune phase of arthritis development, we used the CAIA model. Mice with the NOD-derived *FcγR* gene cluster (*Cia9i* and *Cia9k*) were more susceptible to CAIA, as compared to WT mice (Fig. 3A and B). Disease development before LPS injection, causing antibody-induced

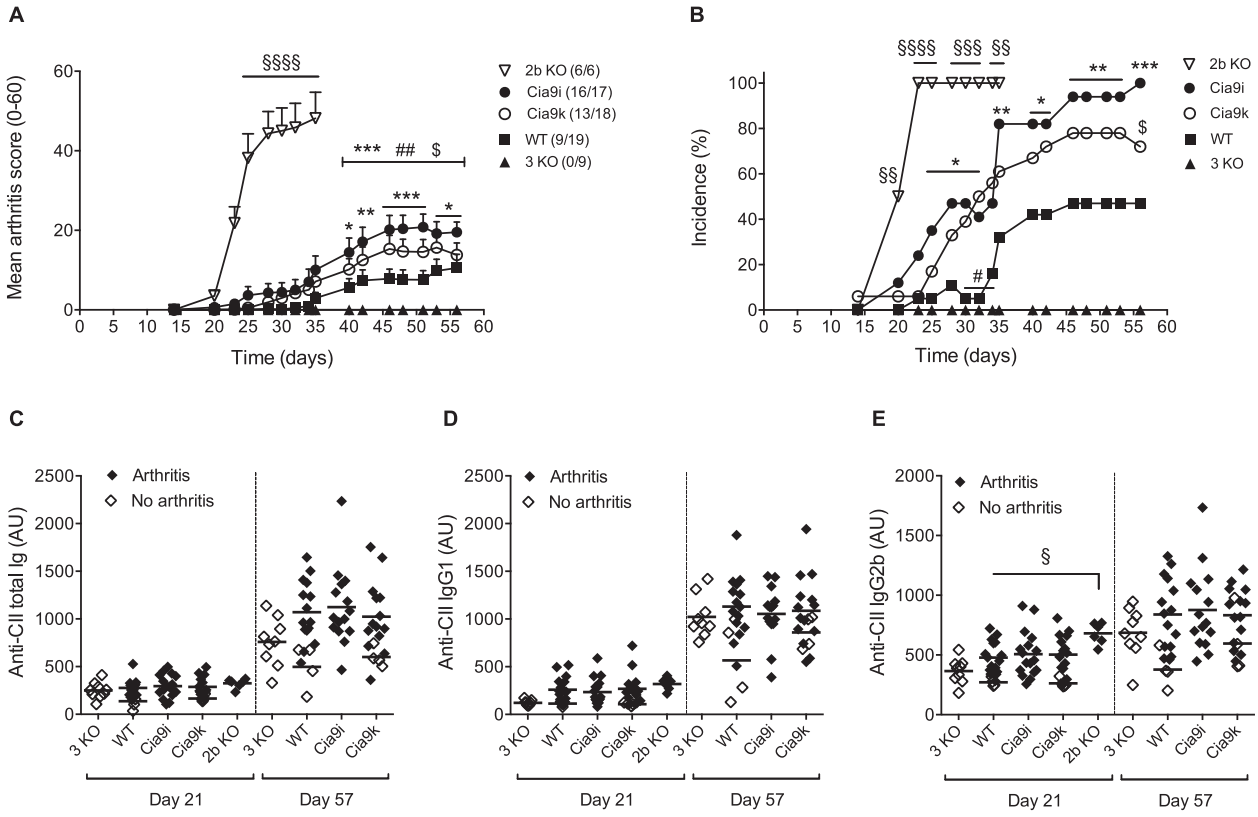

Figure 2. CIA susceptibility of *Cia9i*, *Cia9k* mice, and WT mice. Mice were immunized with CII on day 0 and day 35 and were monitored macroscopically for signs of arthritis. Mean arthritis score (A) and incidence (B) of WT, *Cia9i*, *Cia9k*, FcγR2b KO, and FcγR3 KO mice. FcγR2b KO mice had to be sacrificed on day 35 due to disease severity. At day 21 and day 57 after CIA induction, serum samples were collected to assess total Ig (C), IgG1 (D), and IgG2b (E) levels of anti-CII antibodies, correlated to arthritis development. The values between brackets (A) indicate the number of mice that developed arthritis out of the total number of animals in the experiments. Data show mean + SEM (A) or mean (B–E) and represent pooled data of two individual experiments for WT, *Cia9i*, and *Cia9k* mice. Two-way ANOVA with Tukey's multiple comparison (A), Fisher's exact test among congenics and Chi-Square test for comparison with FcγR2b KO (B) and Mann-Whiney U test (C–E) were used and differences were considered statistically significant when $p < 0.05$ for a 95% confidence interval. Different symbols indicate statistical significance between *Cia9i* and WT mice ($^{*}p < 0.05$, $^{**}p < 0.01$, $^{***}p < 0.001$), *Cia9k* and WT mice ($^{\#}p < 0.05$, $^{\#\#}p < 0.01$), *Cia9i* and *Cia9k* mice ($^{\$}p < 0.05$), and between FcγR2b KO mice and *Cia9i*/*Cia9k*/WT mice ($^{\circ}p < 0.05$, $^{\circ\circ}p < 0.01$, $^{\circ\circ\circ}p < 0.001$, $^{\circ\circ\circ\circ}p < 0.0001$). The flat lines (A,B) indicate multiple timepoints, and the connected line (A) represent the Area under the curve at day 40–56.

joint inflammation, was elevated in *Cia9i* and *Cia9k* congenic mice compared to WT mice (Fig. 3A). This effect was enhanced after LPS stimulation (day 7), increasing inflammatory cell infiltration.

Interestingly, *Cia9i* mice developed arthritis with higher frequency and severity as compared with the *Cia9k* mice. To study a possible FcγR3 independent effect of the congenic fragment, we first investigated ROS-induced phagocytosis of Daudi cells, showing a difference, as compared to WT, by the Cia9i but not the *Cia9k* fragment (Supporting Information Fig. S2A–D). To investigate whether the Cia9i fragment contained other arthritis regulatory genes outside the FcγR cluster, we used the FcγR independent mannan-induced psoriasis (MIP) model [23]. No differences in disease development were observed between *Cia9i* congenic and WT mice (Supporting Information Fig. S2E). Thus, we conclude that there is no other major effect than the FcγR polymorphism in the congenic fragment that could explain the enhanced arthritis seen in both *Cia9i* and *Cia9k*.

No observed effect on B cell function

To investigate why *Cia9i* and *Cia9k* congenic mice were different in arthritis susceptibility, we analyzed the immune cell populations in spleens from naïve mice but found no differences (Supporting Information Fig. S3). A major candidate for the arthritis susceptibility in *Cia9* mice is the *FcγR2b* gene, which is expressed on myeloid cells and B cells, with B cells lacking expression of Fc**γ**R3. It has previously been shown that activated B cells from NOD mice have lower *FcγR2b* expression than C57BL/6.J mice[24]. This is also true for our congenic mice, both gene and protein expression were lower in LPS-activated $CD3^{-}CD19^{+}$ B cells *in vitro* as compared with WT B cells, whereas no differences for naïve B cells were observed (Supporting Information Fig. S4A–C). To determine the ability to produce antibodies in vitro, we stimulated total spleen cells and MACS sorted $CD3^{-}CD19^{+}$ B cells from CIA induced mice *in vitro* with OVA, LPS, CII or medium for 5 days, but no differences in anti-CII antibody pro-

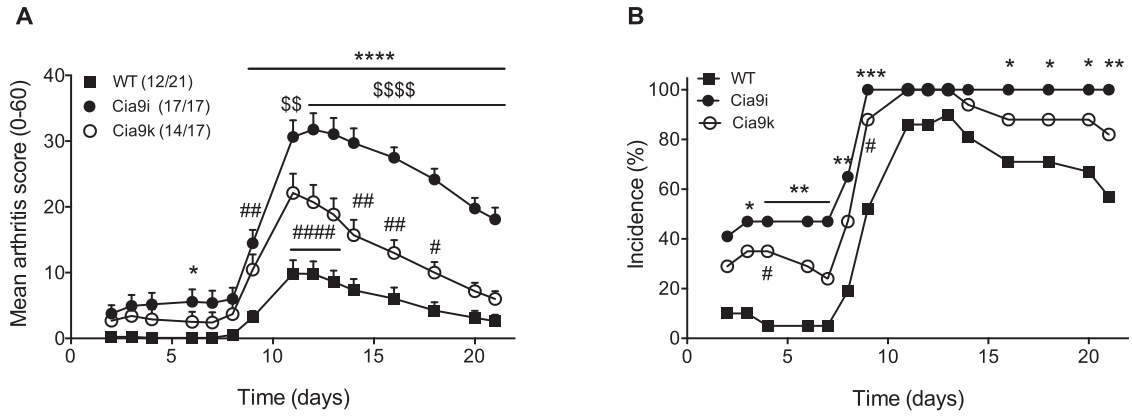

Figure 3. Polymorphisms in the *Cia9i* and *Cia9k* fragment associated with development of antibody-mediated effector phase of arthritis. Mice were injected i.v. with 4 mg of anti-CII mAbs cocktail (M2139+CIIC1+CIIC2+UL1) on day 0 and boosted with LPS i.p. on day 7. Mean arthritis score (A) and incidence (B) of WT, *Cia9i*, and *Cia9k* mice. The values between brackets (A) indicate the number of mice that developed arthritis out of the total number of animals in the experiments. Data show mean+SEM and represent pooled data of two independent experiments. Two-way ANOVA with Tukey's multiple comparison (A) and Fisher's exact test (B) were used and differences were considered statistically significant when $p<0.05$ for a 95% confidence interval. The flat lines indicate multiple timepoints. Differences between WT and *Cia9i* mice: $^{*}p < 0.05$, $^{**}p < 0.01$, $^{***}p < 0.001$, $^{****}p < 0.0001$. Differences between *Cia9i* and *Cia9k* mice: $^{\$\$}p < 0.01$, $^{\$\$\$\$}p < 0.0001$. Differences between WT and *Cia9k* mice $^{\#}p < 0.05$, $^{\#\#}p < 0.01$, $^{\#\#\#\#}p < 0.0001$.

duction between WT and *Cia9i* mice were observed (Supporting Information Fig. S4D).

Despite lower expression of Fc**γ**R2b on activated B cells from *Cia9i* and *Cia9k* mice, no differences in in vitro antibody production by CIA primed B cells were observed, nor could any difference in IgG antibody response after CII immunization be observed (Fig. 2C–E). We conclude that B cells may not be a major mediator of the *FcγR* gene cluster regulated control of arthritis development.

Increased FcγR3 expression on *Cia9i* macrophages regulates effector function

To determine the Fc**γ**R2b expression on macrophages, we isolated thioglycolate-elicited peritoneal macrophages (TpMFs) and analyzed gene and protein expression (Figs. 4A–F). The *FcγR2b* gene expression was drastically reduced in TpMFs of *Cia9i* and *Cia9k* congenic mice compared to WT mice. Both *Cia9i* and *Cia9k* mice had lower Fc**γ**R2b protein expression on un-stimulated and *in vitro* LPS stimulated TpMFs. We also observed elevated gene expression of *Fc**γ**R3* on macrophages from *Cia9i* mice compared to WT. Moreover, elevated levels of Fc**γ**R3 protein were found on *Cia9i* TpMFs compared to WT and *Cia9k* TpMFs, whereas *Cia9k* mice showed lower Fc**γ**R3 protein expression on *in vitro* LPS stimulated TpMFs compared to WT TpMFs. No differences in FcγR4 gene or protein expression levels were observed between NOD and B10.Q-derived congenics. These gene and protein expression differences of the individual Fc**γ**Rs between genotypes were also found on naïve macrophages (Supporting Information Fig. S5).

To determine how the observed Fc**γ**R protein expression affects Fc**γ**R mediated function on macrophages, we used a phagocytosis model. It is known that binding of activating Fc**γ**Rs (Fc**γ**R3 and FcγR4), with pathogen-bound IgG, directly mediates clearance of the pathogen by degranulation of cytotoxic cells and phagocytosis, whereas FcγR2b inhibits the function of activating FcγRs [25]. With the *Cia9k* congenic mouse, excluding NOD FcγR3, we investigated antibody-dependent cellular phagocytosis (ADCP) of rituximab labeled Daudi cells by macrophages from WT, *Cia9i* and *Cia9k* mice, using FcγR3 KO mice as control (Fig. 4G). Here we show that *Cia9i* macrophages, with increased FcγR3 expression, induced more phagocytosis compared to *Cia9k* and WT macrophages (Fig. 4H). As expected, phagocytosis by FcγR3 KO macrophages was reduced compared to that of the congenic macrophages.

We next compared the efficiency of FcγR mediated phagocytosis *in vivo* through depletion of regulatory T (Treg) cells with the anti-CD25 antibody PC61, which is known to be dependent on FcγR3 but not FcγR2b [26]. We found that PC61 reduced the frequency of $CD4^{+}Foxp3^{+}$ Treg cells in peripheral blood in WT, *Cia9i, Cia9k*, and FcγR2b KO mice, but not in FcγR3 KO mice (Supporting Information Fig. S6A–C). Interestingly, the data correlates with our FcγR3 expression data for *Cia9i* macrophages. *Cia9k* mice with lower expression of FcγR, showed less efficient Treg cell depletion even when compared to WT mice. This effect was less pronounced in spleen cells 6 days after PC61 Ab. Nevertheless, both WT mice and *Cia9i* mice showed a reduction in $CD4^{+}Foxp3^{+}$ Treg cell levels compared to naïve mice. Moreover, *Cia9i* mice had fewer $CD4^{+}Foxp3^{+}$ Tregs in the spleen 6 days after PC61 Ab compared to WT and *Cia9k* mice (Supporting Information Fig. S6D–E).

Taken together, *Cia9i* and *Cia9k* macrophages had decreased expression of FcγR2b compared to that of WT mice, whereas *Cia9i* macrophages showed higher expression of FcγR3, which led to increased in vitro and in vivo phagocytosis.

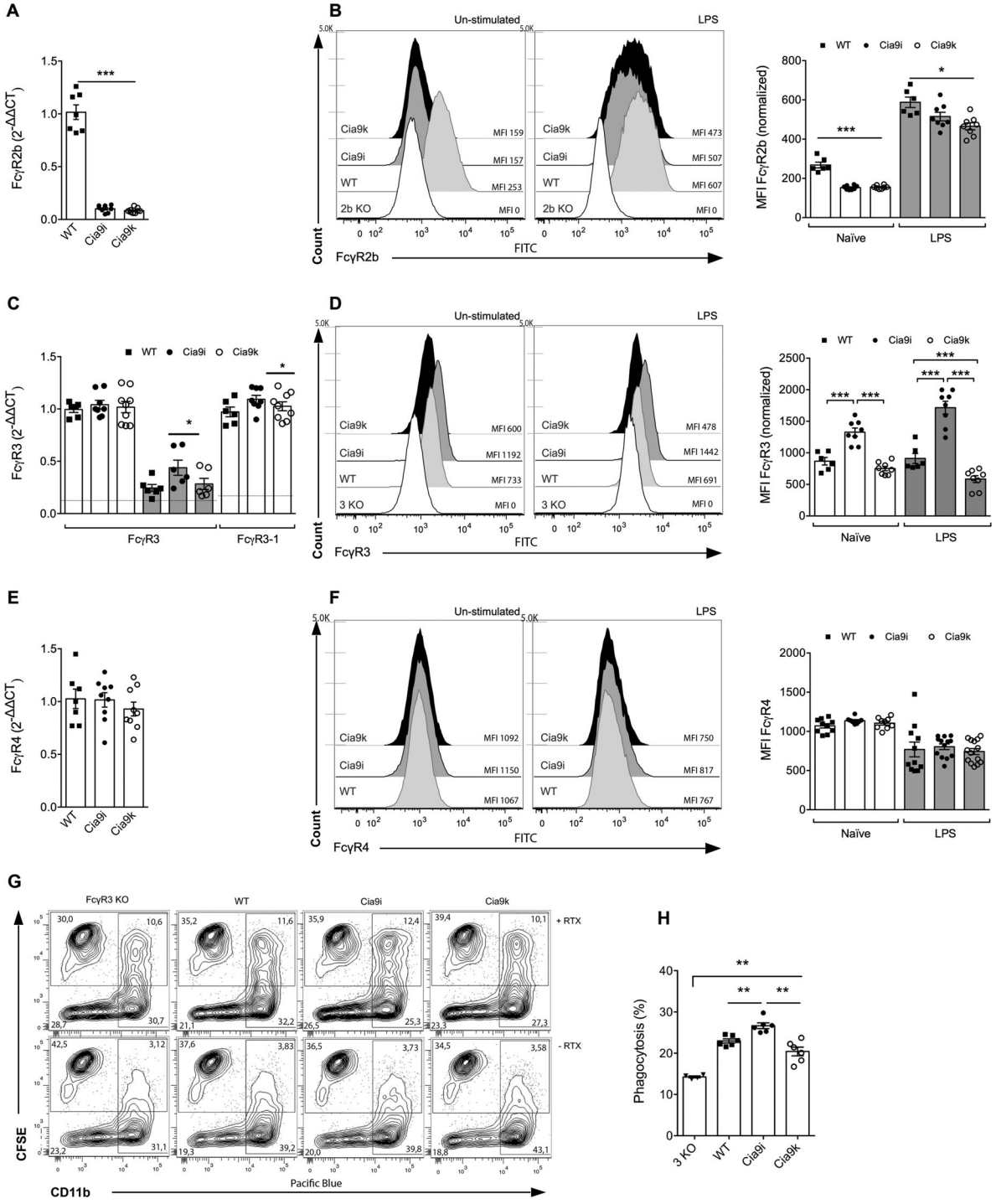

Figure 4. **FcγR3 expression levels on macrophages regulation of antibody-dependent cellular phagocytosis (ADCP).** **(A–F)** Gene and protein expression of FcγR2b (A,B), FcγR3 (C,D), and FcγR4 (E,F) on thioglycollate-elicited peritoneal macrophages (TpMFs) ($CD11b^+F4/80^+$). **(A,E)** WT $n = 7$, *Cia9i* $n = 9$, *Cia9k* $n = 9$. **(A)** Gene expression of *FcγR2b* on FcγR2b KO mice ($n = 6$) was absent. **(C)** *FcγR3* gene expression using primer/probe sets spanning exon boundary 2–3 (FcγR3) and 1–2 (FcγR3-1) on un-stimulated (blank; WT $n = 6$, *Cia9i* $n = 8$, *Cia9k* $n = 9$) or *in vitro* LPS stimulated (grey; $n = 6$) TpMFs. Horizontal line represents gene expression of FcγR3 KO mice ($n = 4$). **(B,D,F)** Representative histogram overlay and normalized protein expression of FcγR2b (B), FcγR3 (D), and FcγR4 (F) on un-stimulated (left) and *in vitro* LPS stimulated (right) TpMFs. **(B, D)** FcγR2b (B) and FcγR3 (D) protein expression were normalized using the MFI from the respective KO mice. WT $n = 6$, *Cia9i* $n = 8$, *Cia9k* $n = 8$. **(F)** Un-stimulated: WT $n = 10$, *Cia9i* $n = 9$, *Cia9k* $n = 9$. LPS: WT $n = 11$, *Cia9i* $n = 13$, *Cia9k* $n = 13$. **(G)** ADCP, Representative flow cytometry contour plots show phagocytosis of Daudi cells ($CD11b^+CFSE^+$) among total Daudi cells ($CFSE^+$) with (+RTX, top) and without (-RTX, bottom) rituximab by macrophages of FcγR3 KO, WT, *Cia9i*, and *Cia9k* mice. **(H)** Phagocytosis of Daudi cells. FcγR3 KO (3 KO) $n = 4$, WT $n = 6$, *Cia9i* $n = 6$, *Cia9i* $n = 6$. The data show mean ± SEM and represent a pool of two (A-E,H) and three (F) individual experiments. (A,C,E) Mann–Whitney *U* test was used and differences were considered statistically significant when $p < 0.05$ for a 95% confidence interval. $^*p < 0.05$, $^{**}p < 0.01$, $^{***}p < 0.001$.

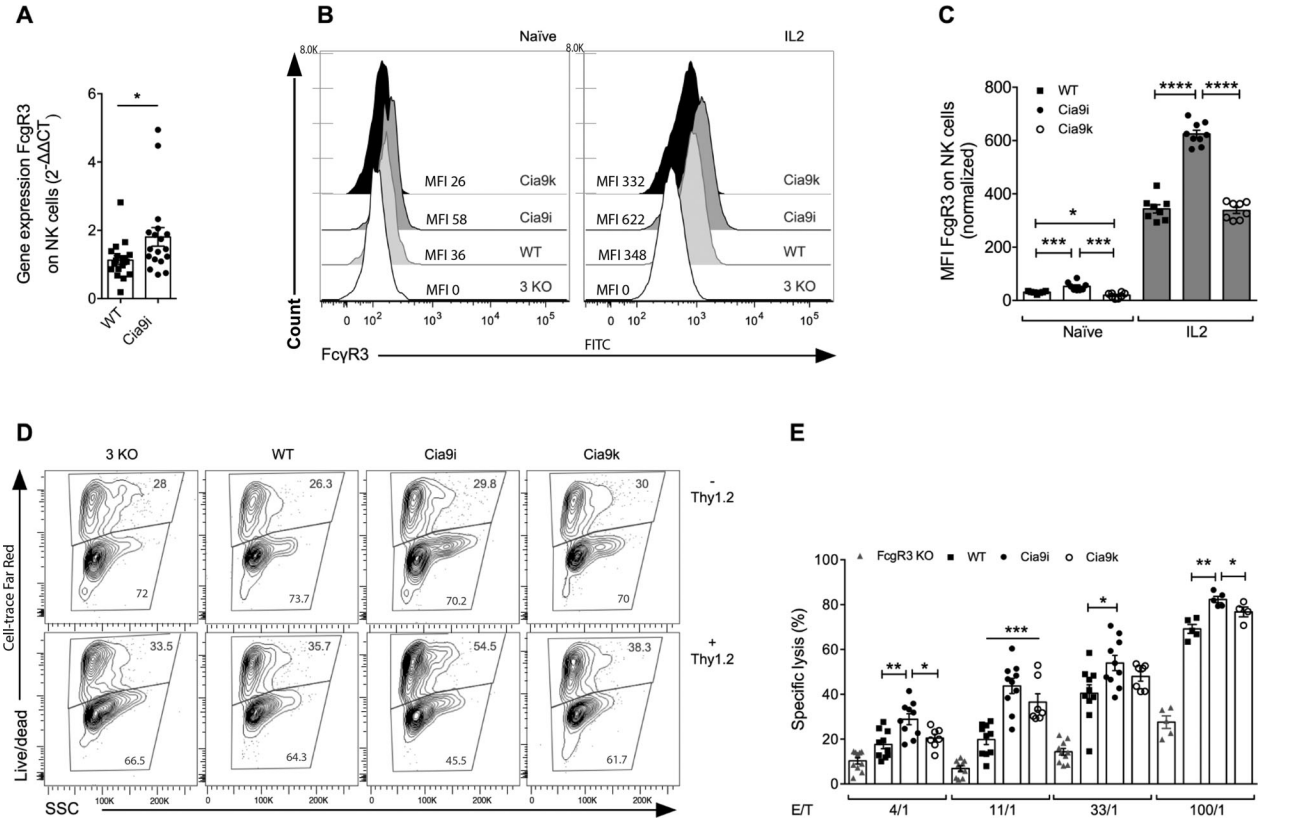

Figure 5. FcγR3 on NK cells regulating cytotoxicity. (A) Gene expression of *FcγR3* on NK cells isolated from spleens of CIA primed WT ($n = 19$) and *Cia9i* congenic mice ($n = 18$) on day 28 after CIA induction. (B) Representative histogram overlay of FcγR3 protein expression on $CD3^-NKp46^+$ NK cells of naïve (left) and IL2 stimulated (right) spleen cells from *Cia9k*, WT, *Cia9i* mice, and FcγR3 KO mice. (C) FcγR3 protein expression shown as MFI on $CD3^-NKp46^+$ NK cells of naïve or IL2 stimulated spleen cells, normalized using the MFI from FcγR3 KO mice. WT n = 8, *Cia9i* n = 9, *Cia9k* n = 8. D) ADCC of RMA cells by IL2 activated NK effector cells. Percentage of killed RMA cells at effector/target ratio (E/T) 4/1 in the absence (top) and presence (bottom) of anti-Thy1.2 antibody. E) Specific lysis of RMA target cells by IL2 activated NK cells at E/T ratio 4/1, 11/1, 33/1 and 100/1. FcγR3 KO mice were used as assay control. FcγR3 KO n = 10, WT n = 10, *Cia9i* n = 10, *Cia9k* n = 7. The data shown are mean ± SEM and represent a pool of 2 (C,E) and 3 (A) independent experiments. E/T 100/1 in (E) represents 1 individual experiment. Mann–Whitney *U* test was used and differences were considered statistically significant when $p < 0.05$ for a 95% confidence interval. $^*p < 0.05$, $^{**}p < 0.01$, $^{***}p < 0.001$, $^{****}p < 0.0001$.

NK cell function is altered by polymorphisms in FcγR3

Since our data indicated a role for FcγR3 in the enhanced arthritis susceptibility of *Cia9i* mice, we next studied NK cell function, solely expressing FcγR3. We found increased *FcγR3* gene expression on CIA primed NK cells of *Cia9i* mice (Fig. 5A). Moreover, FcγR3 protein expression was upregulated in naïve and IL2 activated NK cells from *Cia9i* mice, whereas *Cia9k* mice showed lower FcγR3 protein expression compared to WT mice (Fig. 5B and C). IL-2 activated NK cells were used for FcγR3 mediated antibody-dependent cell cytotoxicity (ADCC) assays, with *Cia9i* NK cells showing more specific lysis at different effector/target ratios (E/T) compared to *Cia9k* and WT mice (Fig. 5D and E). The strains had similar NK cell frequencies and secreted similar amounts of IFNγ upon PMA/ionomycin activation of NK cells (Supporting Information Fig. S7).

These data show that activated NK cells from *Cia9i* mice have upregulated FcγR3 resulting in higher NK cell functionality compared to WT and *Cia9k* mice, arguing for a role for the *FcγR3* polymorphism.

Discussion

The low-affinity FcγR cluster is located in a conserved haplotype with a strong influence on autoimmune diseases. Here, we have identified the underlying polymorphisms in this haplotype by splitting the effect of the closely linked *FcγR2b* and *FcγR3* genes in congenic mouse strains, *Cia9i* and *Cia9k*. This strategy identified both *FcγR2b* and *FcγR3* as regulators of experimental arthritis, regulating independently of each other but contributing to arthritis development additively. Moreover, both genes from the conserved haplotype of *mus musculus musculus* promoted a pro-inflammatory effect as compared to the corresponding haplotype from *mus musculus molossinus* in the B10 mouse.

The FcγRs play an essential role in inflammation and immune response and their functions are quite complex in different pathophysiologic settings. Although nomenclature differs between mice and humans, their function and binding specificities are remarkably similar [27]. The FcγR genes are highly polymorphic and associated with autoimmune diseases. In humans, it has been difficult to identify a disease regulatory polymorphism of *FcγR2a*

and *FcγR2b*, orthologue of mouse *FcγR3* and *FcγR2b*, due to a high degree of linkage disequilibrium. Of particular interest is that in the mouse the three low to intermediate FcγRs (*FcγR2b*, *FcγR3*, and *FcγR4*) are also strongly linked and inherited in a well-conserved haplotype. In fact, different subspecies of wild mice have different haplotypes, and inbred mouse strains have inherited different wild mouse-derived haplotypes [13, 22, 28]. The haplotype polymorphisms could be older than the mouse species as has been suggested for the adjacent SLAM locus [11, 29]. The haplotype from the *Mus musculus musculus*, common on the Eurasia continent, is today carried by NOD, MRL and NZB strains, which are often more susceptible to various autoimmune diseases. In contrast, the C57.Black strains carry a haplotype from the *Mus musculus molossinus,* which naturally occurs on the Japanese islands [28, 30]. The occurrence of different haplotypes in inbred strains can help to understand the biological role of FcγR, in particular since the locus in the human population is also polymorphic. To better understand the biologic impact of this genetic information, it is necessary to isolate and study the effect of the conserved haplotype as well as to split the haplotype in order to investigate the effect of single genes.

Using *Cia9* congenic mice, we initially found that CIA severity and the levels of anti-CII IgG1 antibodies were significantly increased in *Cia9* congenic mice compared to littermate control mice, which mapped to the NOD FcγR locus [14]. However, since the *Cia9* locus consisted of more than 150 genes, the impact of NOD-derived genes other than *FcγR2b* could not be excluded. Aside from the FcγR gene cluster, *Cia9* also contained the SLAM/CD2 gene cluster, which is important in maintaining tolerance in autoimmune diseases and has been linked to lupus [6, 10]. No effect on arthritis development in congenic mice devoid of the FcγR gene cluster was observed, ruling out the role of the big SLAM/CD2 gene cluster in disease development, and the disease regulatory gene(s) were isolated to the *FcγR* region. A split recombination within the region showed that the *FcγR2b* and *FcγR3* genes jointly and additively cause the effect on arthritis. However, we cannot exclude an influence of additional genes within these small fragments. Luan *et al.* [24] described several effects contrasting to the present data but these variabilities are most likely dependent on the older data being based on a very large (25 cM) congenic fragment containing many other immune regulatory genes. Another limitation of the study is that we have not explored the full potential of the FcgR polymorphism on inflammatory responses as we have only investigated selected disease models, activation inducers, and cell types.

With the recombination between the *FcγR2b* and the *FcγR3* loci, we were able to study the single effect of FcγR2b and the combined effect of FcγR2b and FcγR3 on inflammatory responses. We showed that the FcγR2b and FcγR3 alleles operated in concert with an additive effect and primarily controlled the inflammatory effector phase of arthritis, but not the priming autoimmune phase.

To further investigate the role of polymorphic *FcγR2b* and *FcγR3*, FcγR-dependent functions on B cells, NK cells, and macrophages were studied. Impaired FcγR2b expression in B cells in mice has been shown to influence antibody production in an antigen-independent manner [31]. Despite lower expression of FcγR2b on *Cia9i* and *Cia9k in vitro* activated B cells, no significant differences in anti-CII antibody secretion were observed. In contrast, the increased expression of FcγR3 derived from the NOD allele are likely to play a role in arthritis and showed a more pronounced phagocytosis *in vitro* and *in vivo*.

Nevertheless, despite the dramatic reduction of the arthritis prone congenic fragment there are still some additional genes in the FcγR gene cluster flanking region that might impact downstream functions. This has been indicated by the altered NK cell killing function in the *Cia9k* mice with an isolated NOD derived *FcγR2b* allele. Whereas the specific lysis by *Cia9i* and WT NK cells was linked to FcγR3 expression, that of *Cia9k* NK cells was not. Since FcγR3 expression in *Cia9k* NK cells was slightly reduced compared to WT NK cells, we expected lower or equal NK cell-mediated lysis. Interestingly though, specific lysis by *Cia9k* NK cells was lower than that of *Cia9i* NK cells, but increased compared to that of WT NK cells. This implies possible involvement of other linked genes within the congenic fragment. The only gene within the *Cia9k* fragment that has been associated with NK cell-medicated cytotoxicity is the activating transcription factor 6 (Atf6) [32]. It is possible that without NOD.Q FcγR3, NOD.Q Atf6 still controls cytotoxicity. Nonetheless, with our congenic mice, we were able to study the independent and additive effect of FcγR2b and FcγR3 on inflammation. Our congenic mice could provide a more physiological setting to study FcγR function.

In summary, we found that it is indeed the FcγR gene cluster of the *Cia9* region that controls chronic inflammation, and that FcγR3 polymorphism on macrophage regulate effector functions. To conclude, it is the additive effect of genetic polymorphisms in *FcγR2b* and *FcγR3* that regulate inflammation, most likely due to natural haplotype selection.

Materials and methods

Mice

Mice were bred and kept at the Karolinska Institute in Stockholm, Sweden (a specific pathogenic free unit with intraventilated cages). We used the 10-Mb *Cia9* congenic fragment [14], to generate the sub-congenic fragments derived from NOD on to the B10.Q background (Fig. 1). FcγR2b KO [33] and FcγR3 KO mice [34], generated by gene targeting in 129-derived ES cells and backcrossed for more than ten generations to C57BL/6.J, were obtained from Jackson Laboratory. They were further backcrossed into B10.Q background for more than ten generations in the MIR animal house and were used as experimental controls for various assays. Genotyping was performed using markers shown in Supporting Information Table S2. Haplotype variation analysis in the genomic region (170.9–171.07Mbp) that harbors FcγR2b, FcγR4, and FcγR3 is based on 4020 SNPs found in the Welcome Trust mouse genome project database (Welcome Sanger Institute, UK),

comparing sequencing-data from 37 different mouse genomes, including the reference genome C57BL/6J [21].

All experimental animal procedures were approved by the local ethics committees and were performed using B10.Q WT littermate control mice. All experiments were performed in a blinded manner with age- and sex-matched groups randomly distributed in cages. Unless stated otherwise, 10–12 weeks old male mice were used for *in vivo* experiments. Animal model experiments, including serologic measurement, were performed following earlier described protocols for CIA [14], CAIA [16], and MIP [23].

Cells and antibodies

The RMA T leukemia cell line, used for NK cell-mediated killing, was provided by Dr. M. Johansson (Karolinska Institute, Stockholm, Sweden) and the Daudi human B cell lymphoma cell line was provided by Dr. N. Nagy (MTC, Karolinska Institute, Stockholm, Sweden). The following antibodies were purchased from BD Biosciences (San Jose, CA) or Biolegend (San Diego, CA) and were used for analysis on a LSR-II flow cytometer (BD Biosciences): anti-CD45 (30-F11), -CD3 (145-2C11), -TCRβ (H57-597), -CD4 (H129.19), -CD8 (53-6.7), -CD19 (6D5), -CD45R/B220 (RA3-6B2), -NK1.1 (PK136), -NKp46 (29A1.4), -CD25 (PC61.5), -CD11b (M1/70), F4/80 (BM8), -CD11c (HL3), -GR-1 (RB6-8C5), and -IFN (R46A2). Antibodies to iNOS (eBR2a) and Foxp3 (FJK-16S) were from eBioscience (San Diego, CA). The FITC-conjugated anti-mouse FcγR antibodies: anti-FcγR2b (AT130-2), -FcγR3 (AT154-2) and -FcγR4 (AT137), were generated in Southampton as previously described [35]), and were used at 10, 20, and 10 μg/ml, respectively. Viability of the cells was determined with LIVE/DEAD fixable near-IR or violet dead cell stain kit (Invitrogen, Carlsbad, CA). Cancer cells were labeled with CellTrace CFSE or CellTrace Violet cell proliferation kit (Invitrogen, Carlsbad, CA). Data analysis was performed using the FlowJo software (TreeStar).

Quantitative real-time PCR

Total RNA was extracted using Trizol and the PureLink RNA Mini Kit (Ambion, Thermo Fisher Scientific, Waltham, MA, Life Technologies, Inc., Foster City, CA). RNA was reverse transcribed to cDNA using the High Capacity cDNA Reverse Transcription Kit (ABI Applied Biosystems, Foster City, CA). Quantitative real-time PCR (qRT-PCR) was performed on a Bio-Rad CFX96 System (Hercules, CA, USA) using TaqMan™ according to the manufacturer's protocol. TaqMan® Gene Expression Assays (Thermo Fisher Scientific) for FcγR2b (Mm00438875_m1 FAM), FcγR3 (Mm00438882-m1 FAM, primers/probe spanning exon2-3), FcγR3-1 (Mm01290524-m1 FAM, primers/probe spanning exon1-2), FcγR4 (Mm00519988_m1 FAM), and the housekeeping genes Actin-β (Mm00607939_s1 VIC) and GAPDH (Mm99999915_g1 VIC) were used. The relative expression of each FcγR gene was determined after normalization to both housekeeping genes and samples from naïve WT mice using the ΔΔCt method.

B cell analysis

Spleens were harvested and processed into single-cell suspensions and B cells enriched by positive selection through CD19 microbeads according to the manufacturer's protocol (MACS, Miltenyi Biotec, Bergisch Gladback, Germany). The purified B cells ($CD3^-CD19^+$) were determined to be >90% purity by flow cytometric analysis and used for culture and qRT-PCR.

Purified B cells and whole splenocytes were cultured in DMEM (Gibco, Thermo Fisher) supplemented with 50 U/ml penicillin, 50 mg/ml streptomycin, 10% HI fetal bovine serum, 50 μM β-mercaptoethanol, and 10 mM HEPES buffer (complete DMEM) in the presence of 10 μM LPS, 10 μM CII, 10 μM OVA, or medium alone. Cells were stimulated for 5 days in 5% CO_2 at 37°C and anti-CII Ab production was detected by ELISA using HRP conjugated anti-kappa mAb as described above.

FcγR2b protein expression was determined on $CD3^-CD19^+$ or $CD3^-CD45R^+$ cells, on total spleen cells and purified B cells, from naïve *Cia9i*, *Cia9k*, and WT mice, using flow cytometry analysis of FITC conjugated anti-FcγR2b (AT130-2, 10 μg/ml). All flow cytometyric analysis followed published guidelines [36]. Cells were stimulated with LPS for 20 h to activate B cells or left unstimulated. FcγR2b KO mice were used as control. FcγR2b gene expression was determined on purified B cells and LPS-stimulated B cells using qRT-PCR as well.

Macrophage analysis

Macrophages were collected by peritoneal lavage or differentiated from BM cells. Naïve mice were injected i.p. with 1 ml 3–4% Brewer's thioglycollate (Difco, BD) and peritoneal lavage were taken 4–5 days after. For qRT-PCR, cells were allowed to adhere to the surface of culture plates for 1–2 h in DMEM supplemented with 50 U/ml penicillin, 50 μg/ml streptomycin, and 10% HI FCS. Non-adherent cells were washed away and the adherent cells were treated with Trizol for RNA extraction. The adherent cells consisted of more than 90% $F4/80^+CD11b^+$ cells, confirmed by flow cytometry analysis.

For BM-derived macrophages (BMM), femurs were flushed and cells were cultured at 1.25×10^5 cells/ml in complete DMEM containing M-CSF for 7 days in 5% CO^2 at 37°C. All cells were $F4/80^+CD11b^+$. Thioglycollate-elicited macrophages (TpMFs) and BMMs were used for flow cytometry analysis of FcγR proteins and for antibody-dependent cellular phagocytosis (ADCP). For ADCP, cells were cultured in DMEM, 10% FCS at 37°C, 5% CO_2, and allowed to adhere ON.

Peritoneal cells were cultured in complete DMEM with or without 1 μg/ml LPS for 20 hours at 37°C, 5% CO^2. Macrophages were stained with FITC-conjugated anti-mouse FcγR2b (AT130-2), FcγR3 (AT154-2), or FcγR4 (AT137) antibodies on $F4/80^+CD11b^+$ pMQs and analyzed on a flow cytometer.

Expression was measured as the MFI for each FcγR, using FcγR2b KO and FcγR3 KO mice as control for FcγR2b and FcγR3 expression, respectively. Oxidative burst assays were performed as earlier described [9].

Antibody-dependent cellular phagocytosis

Antibody-dependent cellular phagocytosis (ADCP) was determined by flow cytometry. Macrophages were seeded at 5×10^4 cells/well into 96-well plates ON. Target Daudi cells were labeled with 5 μM CellTrace™ CFSE for 5 min at 37°C and quenched with FCS for 5 minutes at room temperature. Cells were washed twice with pre-warmed culture medium and resuspended in culture medium. Labeled Daudi cells were added to the macrophages at a 5/1 E/T ratio with or without rituximab (RTX) (provided by Inger Gjertsson, Rheumatology Unit, Sahlgrenska Hospital, Göteborg, Sweden) at 1 μg/ml for 4 h in 5% CO_2 at 37°C. After 4 h, cells were stained with F4/80 and CD11b and analyzed. ADCP was defined as the percentage of macrophages that had phagocytized. Phagocytosis was calculated as the percentage macrophages ($CFSE^+$ $CD11b^+$) among total target cells ($CFSE^+$) per sample with and without RTX, and was normalized using the no RTX sample as negative control: (RTX sample – no RTX control) / (100% – no RTX control) × 100%.

NK cell culture

NK cells for qRT-PCR were isolated from spleens of CIA induced *Cia9i* and WT mice. Non-NK cells were labeled with a cocktail of biotin-conjugated antibodies and anti-biotin microbeads from the MACS NK cell isolation kit II, leaving unlabeled NK cells.

To activate NK cells, splenocytes from naïve *Cia9i, Cia9k*, WT, and FcγR3 KO mice were cultured for 4–7 days in complete α-MEM (containing 50 U/ml penicillin, 50 mg/ml streptomycin, 50 μM β-ME, 10 mM HEPES, 1 mM sodium pyruvate, 2 mM L-glutamine, and 10% HI FCS) supplemented with human rIL-2 (1000 U/ml; PeproTech) in 7% CO_2 at 37°C [37]. These cells were used as effector cells in antibody-dependent cell-mediated cytotoxicity (ADCC) assays.

FcγR3 protein expression was assessed on $CD3^-NKp46^+$ naïve spleen cells and IL2 stimulated splenocytes, using flow cytometry analysis of FITC conjugated anti-FcγR3 (AT154-2, 20 μg/ml). Expression was measured as the MFI, using FcγR3 KO mice as control.

Antibody-dependent cell-mediated cytotoxicity by NK cells

RMA cells were labeled with 5 μM CellTrace™ CFSE or CellTrace™ Violet (CTV) as described above. Labeled RMA cells were used as target cells at 5×10^3 cells per well in 96-well round-bottom plates and pre-incubated with 5 μg/ml anti-Thy1.2 (clone 30-H12, BD) for 10 min at 37°C, and washed with complete α-MEM. NK effector cells were added to the wells containing RMA cells at effector/target (E/T) ratios 4/1, 11/1, 33/1, and 100/1 and incubated at 37°C for 4 h [37]. To determine the background cytotoxicity, culture medium instead of anti-Thy1.2 was added as negative control. As positive control, target cells were heated for 30 minutes at 45°C [38]. ADCC was determined by flow cytometry. Cells were labeled with a fixable viability dye and NK cell ($CD3^-NKp46^+$) markers. Specific lysis was calculated with the number of tumor target cells killed per sample: (experimental sample – negative control) / (positive control – negative control) × 100%.

In vivo regulatory T cell depletion

$CD25^+$ Treg cells were depleted *in vivo* using PC61.5 Ab [26, 39]. One day before Treg cell depletion, *Cia9i, Cia9k,* WT, FcγR2b KO and FcγR3 KO mice were bled by tail bleeding to establish their baseline $CD4^+Foxp3^+$ T cell population. At day 0, mice were injected i.p. with 250 μg anti-CD25 (PC61.5) mAb. Blood was collected at day 1 and day 3 after PC61 Ab to determine the frequency of $CD4^+Foxp3^+$ T cells. At day 3, mice were given a second injection of 250 μg PC61. Peripheral blood and spleens were collected at day 6 after PC61 Ab and analyzed by flow cytometry for $TCR\beta^+$/ $CD4^+Foxp3^+$ cells.

Statistical analysis

GraphPad Prism software (San Diego, CA, USA) was used for statistical analysis. Arthritis severity and incidence between the groups of animals were analyzed using Two-way ANOVA with Tukey's multiple comparison and the Fisher's exact test (and Chi-Square test when comparing to FcγR2b KO mice) respectively. For all *in vitro* experiments, the Mann-Whitney *U* test was used when comparing data from two groups. Significance was considered when $P<0.05$ for a 95% confidence interval.

Acknowledgments: We would like to thank Dr. Michael Förster for help with the *Cia9* mice, Dr. Ia Khmaladze for help with the hybridomas, Dr. Inger Gjertsson for providing us with rituximab, Dr. Maria Johansson for their RMA cell line, Dr. Naomi Nagy for their Daudi cell lines, and the personnel of the animal facility (MIR) at KI for their excellent animal care. This work was supported by grants from Marie Curie Fellowship Network (Osteoimmune, EU FP7-MC-ITN-289150), by the Swedish Research Council, Ehrling Persson Science foundation, Knut and Alice Wallenberg Foundation, and the EU IMI project RTCure.

Conflict of Interest: The authors declare no commercial or financial conflict of interest.

Peer review: The peer review history for this article is available at https://publons.com/publon/10.1002/eji.202048605.

References

1 **Franke, L., el Bannoudi, H., Jansen, D. T., Kok, K., Trynka, G., Diogo, D., Swertz, M. et al.,** Association analysis of copy numbers of FC-gamma receptor genes for rheumatoid arthritis and other immune-mediated phenotypes. *Eur. J. Hum. Genet.* 2016. **24**: 263–270.

2 **Gillis, C., Gouel-Cheron, A., Jonsson, F. and Bruhns, P.,** Contribution of Human FcgammaRs to Disease with Evidence from Human Polymorphisms and Transgenic Animal Studies. *Front Immunol* 2014. **5**: 254.

3 **Johansson, Å. C. M., Sundler, M., Kjellen, P., Johannesson, M., Cook, A., Lindqvist, A. K., Nakken, B. et al.,** Genetic control of collagen-induced arthritis in a cross with NOD and C57BL/10 mice is dependent on gene regions encoding complement factor 5 and FcgammaRIIb and is not associated with loci controlling diabetes. *Eur J Immunol* 2001. **31**: 1847–1856.

4 **Jiang, Y., Hirose, S., Sanokawa-Akakura, R., Abe, M., Mi, X., Li, N., Miura, Y. et al.,** Genetically determined aberrant down-regulation of FcgammaRIIB1 in germinal center B cells associated with hyper-IgG and IgG autoantibodies in murine systemic lupus erythematosus. *Int Immunol* 1999. **11**: 1685–1691.

5 **Morel, L., Blenman, K. R., Croker, B. P. and Wakeland, E. K.,** The major murine systemic lupus erythematosus susceptibility locus, Sle1, is a cluster of functionally related genes. *Proc Natl Acad Sci U S A* 2001. **98**: 1787–1792.

6 **Wandstrat, A. E., Nguyen, C., Limaye, N., Chan, A. Y., Subramanian, S., Tian, X. H., Yim, Y. S. et al.,** Association of extensive polymorphisms in the SLAM/CD2 gene cluster with murine lupus. *Immunity* 2004. **21**: 769–780.

7 **Sato-Hayashizaki, A., Ohtsuji, M., Lin, Q., Hou, R., Ohtsuji, N., Nishikawa, K., Tsurui, H. et al.,** Presumptive role of 129 strain-derived Sle16 locus in rheumatoid arthritis in a new mouse model with Fcgamma receptor type IIb-deficient C57BL/6 genetic background. *Arthritis Rheum* 2011. **63**: 2930–2938.

8 **Boross, P., Arandhara, V. L., Martin-Ramirez, J., Santiago-Raber, M. L., Carlucci, F., Flierman, R., van der Kaa, J. et al.,** The inhibiting Fc receptor for IgG, FcgammaRIIB, is a modifier of autoimmune susceptibility. *J Immunol* 2011. **187**: 1304–1313.

9 **Sareila, O., Hagert, C., Rantakari, P., Poutanen, M. and Holmdahl, R.,** Direct Comparison of a Natural Loss-Of-Function Single Nucleotide Polymorphism with a Targeted Deletion in the Ncf1 Gene Reveals Different Phenotypes. *PLoS One* 2015. **10**: e0141974.

10 **Morel, L., Rudofsky, U. H., Longmate, J. A., Schiffenbauer, J. and Wakeland, E. K.,** Polygenic control of susceptibility to murine systemic lupus erythematosus. *Immunity* 1994. **1**: 219–229.

11 **Limaye, N., Belobrajdic, K. A., Wandstrat, A. E., Bonhomme, F., Edwards, S. V. and Wakeland, E. K.,** Prevalence and evolutionary origins of autoimmune susceptibility alleles in natural mouse populations. *Genes Immun* 2008. **9**: 61–68.

12 **Cornall, R. J., Prins, J.-B., Todd, J. A., Pressey, A., DeLarato, N. H., Peterson, L., Wicker, L. S. et al.,** Type 1 diabetes in mice is linked to the interleukin-1 receptor and Lsh/Ity/Bcg genes on chromosome 1. *Nature* 1991. **353**: 262–264.

13 **Ahlqvist, E., Ekman, D., Lindvall, T., Popovic, M., Forster, M., Hultqvist, M., Klaczkowska, D. et al.,** High-resolution mapping of a complex disease, a model for rheumatoid arthritis, using heterogeneous stock mice. *Hum Mol Genet* 2011. **20**: 3031–3041.

14 **Förster, M., Raposo, B., Ekman, D., Klaczkowska, D., Popovic, M., Nandakumar, K. S., Lindvall, T. et al.,** Genetic control of antibody production during collagen-induced arthritis development in heterogeneous stock mice. *Arthritis Rheum* 2012. **64**: 3594–3603.

15 **Holmdahl, R., Rubin, K., Klareskog, L., Larsson, E. and Wigzell, H.,** Characterization of the antibody response in mice with type II collagen-induced arthritis, using monoclonal anti-type II collagen antibodies. *Arthritis Rheum* 1986. **29**: 400–410.

16 **Nandakumar, K. S., Svensson, L. and Holmdahl, R.,** Collagen type II-specific monoclonal antibody-induced arthritis in mice: description of the disease and the influence of age, sex, and genes. *Am J Pathol* 2003. **163**: 1827–1837.

17 **Yuasa, T., Kubo, S., Yoshino, T., Ujike, A., Matsumura, K., Ono, M., Ravetch, J. V. et al.,** Deletion of Fcgamma Receptor IIB Renders H-2(b) Mice Susceptible to Collagen-induced Arthritis. *J Exp Med* 1999. **189**: 187–194.

18 **Kleinau, S., Martinsson, P. and Heyman, B.,** Induction and suppression of collagen-induced arthritis is dependent on distinct fcgamma receptors. *J Exp Med* 2000. **191**: 1611–1616.

19 **Diaz de Stahl, T., Andren, M., Martinsson, P., Verbeek, J. S. and Kleinau, S.,** Expression of FcgammaRIII is required for development of collagen-induced arthritis. *Eur J Immunol* 2002. **32**: 2915–2922.

20 **Nandakumar, K. S., Andren, M., Martinsson, P., Bajtner, E., Hellstrom, S., Holmdahl, R. and Kleinau, S.,** Induction of arthritis by single monoclonal IgG anti-collagen type II antibodies and enhancement of arthritis in mice lacking inhibitory FcgammaRIIB. *Eur J Immunol* 2003. **33**: 2269–2277.

21 **Keane, T. M., Goodstadt, L., Danecek, P., White, M. A., Wong, K., Yalcin, B., Heger, A. et al.,** Mouse genomic variation and its effect on phenotypes and gene regulation. *Nature* 2011. **477**: 289–294.

22 **Espeli, M., Clatworthy, M. R., Bokers, S., Lawlor, K. E., Cutler, A. J., Kontgen, F., Lyons, P. A. et al.,** Analysis of a wild mouse promoter variant reveals a novel role for FcgammaRIIb in the control of the germinal center and autoimmunity. *J Exp Med* 2012. **209**: 2307–2319.

23 **Khmaladze, I., Kelkka, T., Guerard, S., Wing, K., Pizzolla, A., Saxena, A., Lundqvist, K. et al.,** Mannan induces ROS-regulated, IL-17A-dependent psoriasis arthritis-like disease in mice. *Proc Natl Acad Sci U S A* 2014. **111**: E3669–3678.

24 **Luan, J. J., Monteiro, R. C., Sautes, C., Fluteau, G., Eloy, L., Fridman, W. H., Bach, J. F. et al.,** Defective Fc gamma RII gene expression in macrophages of NOD mice: genetic linkage with up-regulation of IgG1 and IgG2b in serum. *J Immunol* 1996. **157**: 4707–4716.

25 **Smith, K. G. and Clatworthy, M. R.,** FcgammaRIIB in autoimmunity and infection: evolutionary and therapeutic implications. *Nat Rev Immunol* 2010. **10**: 328–343.

26 **Setiady, Y. Y., Coccia, J. A. and Park, P. U.,** In vivo depletion of CD4+FOXP3+ Treg cells by the PC61 anti-CD25 monoclonal antibody is mediated by FcgammaRIII+ phagocytes. *Eur J Immunol* 2010. **40**: 780–786.

27 **Dekkers, G., Bentlage, A. E. H., Stegmann, T. C., Howie, H. L., Lissenberg-Thunnissen, S., Zimring, J., Rispens, T. et al.,** Affinity of human IgG subclasses to mouse Fc gamma receptors. *MAbs* 2017. **9**: 767–773.

28 **Takada, T., Yoshiki, A., Obata, Y., Yamazaki, Y. and Shiroishi, T.,** NIG_MoG: a mouse genome navigator for exploring intersubspecific genetic polymorphisms. *Mamm Genome* 2015. **26**: 331–337.

29 **Valdar, W., Solberg, L. C., Gauguier, D., Burnett, S., Klenerman, P., Cookson, W. O., Taylor, M. S. et al.,** Genome-wide genetic association of complex traits in heterogeneous stock mice. *Nat Genet* 2006. **38**: 879–887.

30 **Nunome, M., Ishimori, C., Aplin, K. P., Tsuchiya, K., Yonekawa, H., Moriwaki, K. and Suzuki, H.,** Detection of recombinant haplotypes in wild mice (Mus musculus) provides new insights into the origin of Japanese mice. *Mol Ecol* 2010. **19**: 2474–2489.

31 **Takai, T.**, Fc receptors and their role in immune regulation and autoimmunity. *J Clin Immunol* 2005. **25**: 1–18.

32 **Gong, J.**, **Fang, L.**, **Liu, R.**, **Wang, Y.**, **Xing, J.**, **Chen, Y.**, **Zhuang, R. et al.**, UPR decreases CD226 ligand CD155 expression and sensitivity to NK cell-mediated cytotoxicity in hepatoma cells. *Eur J Immunol* 2014. **44**: 3758–3767.

33 **Takai, T.**, **Ono, M.**, **Hikida, M.**, **Ohmori, H. and Ravetch, J. V.**, Augmented humoral and anaphylactic responses in Fc gamma RII-deficient mice. *Nature* 1996. **379**: 346–349.

34 **Hazenbos, W. L.**, **Gessner, J. E.**, **Hofhuis, F. M.**, **Kuipers, H.**, **Meyer, D.**, **Heijnen, I. A.**, **Schmidt, R. E. et al.**, Impaired IgG-dependent anaphylaxis and Arthus reaction in Fc gamma RIII (CD16) deficient mice. *Immunity* 1996. **5**: 181–188.

35 **Williams, E. L.**, **Tutt, A. L.**, **French, R. R.**, **Chan, H. T.**, **Lau, B.**, **Penfold, C. A.**, **Mockridge, C. I. et al.**, Development and characterisation of monoclonal antibodies specific for the murine inhibitory FcgammaRIIB (CD32B). *Eur J Immunol* 2012. **42**: 2109–2120.

36 **Cossarizza, A.**, **Chang, H. D.**, **Radbruch, A.**, **Acs, A.**, **Adam, D.**, **Adam-Klages, S.**, **Agace, W. W. et al.**, Guidelines for the use of flow cytometry and cell sorting in immunological studies (second edition). *Eur J Immunol* 2019. **49**: 1457–1973.

37 **Wickström, S. L.**, **Öberg, L.**, **Kärre, K. and Johansson, M. H.**, A genetic defect in mice that impairs missing self recognition despite evidence for normal maturation and MHC class I-dependent education of NK cells. *J Immunol* 2014. **192**: 1577–1586.

38 **Salinas-Jazmin, N.**, **Hisaki-Itaya, E. and Velasco-Velazquez, M. A.**, A flow cytometry-based assay for the evaluation of antibody-dependent cell-mediated cytotoxicity (ADCC) in cancer cells. *Methods Mol Biol* 2014. **1165**: 241–252.

39 **Lowenthal, J. W.**, **Corthesy, P.**, **Tougne, C.**, **Lees, R.**, **MacDonald, H. R. and Nabholz, M.**, High and low affinity IL 2 receptors: analysis by IL 2 dissociation rate and reactivity with monoclonal anti-receptor antibody PC61. *J Immunol* 1985. **135**: 3988–3994.

Abbreviations: **CAIA**: collagen antibody-induced arthritis · **CIA**: collagen-induced arthritis · **ES**: embryonic stem · **RA**: rheumatoid arthritis · **SLAM**: signaling lymphocyte activation molecule · **SLE**: systemic lupus erythematosus

Full correspondence: Rikard Holmdahl, MD, PhD, Division of Medical Inflammation Research, Department of Medical Biochemistry and Biophysics, Karolinska Institute, 171 77 Stockholm, Sweden. e-mail: rikard.holmdahl@ki.se

Received: 26/2/2020
Revised: 15/9/2020
Accepted: 13/11/2020
Accepted article online: 26/11/2020